9 Cantilever based gas sensing

HANS PETER LANG

National Center of Competence for Research in Nanoscale Science
Institute of Physics of the University of Basel,
Klingelbergstrasse 82, 4056 Basel, Switzerland
Tel. +41 61 267 3769, Fax. +41 61 267 3795
Email: Hans-Peter.Lang@unibas.ch

Table of Contents

9.1 Introduction to microcantilever based sensing

9.1.1 Early approaches to mechanical sensing

Male individuals of certain animal species like the large domestic silkmoth *bombyx mori*, who is the adult of the silk-thread producing silkworm, are able to detect pheromones emitted by the female over several miles by means of their antennas. Such high sensitivity is achieved by evolution-driven optimization of chemical detection aimed for the survival of a species. A single pheromone molecule already triggers perception. However, a change of behavior only occurs at higher concentration. Highly specific receptors for certain chemical compounds are often based on the geometrical conformation of the target molecule, supported by chemical affinities and binding between specific functional groups. The adsorption process is frequently related to local conformational changes, which are of mechanical nature. Thin membranes and beams also possess mechanical properties that render them suitable for detection of small forces. This fact can be easily demonstrated when water adsorbs on thin membranes, where the large effect of surface tension of water leads to deformation of such thin membranes.

Detecting adsorption by measurement of bending or change in resonance frequency using beams of silicon as sensors was already described by Wilfinger et al [72], who detected resonances in large silicon cantilever structures of 50 mm × 30 mm × 8 mm. Actuation was performed by localized thermal expansion in diffused resistors (piezoresistors) located near the cantilever support to create a temperature gradient that drives the cantilever at its resonance frequency. Similarly, the piezoresistors could also be used to monitor mechanical deflection of the cantilever. Heng [25] fabricated gold microcantilevers capacitively coupled to microstrip lines for mechanical trimming of high-frequency oscillator circuits. Petersen [48] constructed cantilever-type micromechanical membrane switches made from silicon designed to bridge the gap between silicon transistors and mechanical electromagnetic relays. Kolesar [31] suggested the use of cantilever structures as electronic detectors for nerve agents.
The breakthrough for microcantilevers came with the advent of atomic force microscopy (Binnig et al [7]), as microfabricated cantilevers have become easily commercially available. The technical development also triggered research reports of microcantilever use as sensors. Itoh et al [29] presented a microcantilever coated with a thin film of zinc-oxide with piezoresistive deflection readout. Cleveland et al [13] reported the tracking of cantilever resonance frequency to detect nanogram changes in mass loading when small particles are deposited onto AFM probe tips. Gimzewski et al [21] showed first chemical sensing applications, in

which static cantilever bending revealed chemical reactions, such as the platinum-assisted catalytic conversion of hydrogen and oxygen into water at very high sensitivity. Thundat et al [68] demonstrated that the resonance frequency as well as static bending of microcantilevers is influenced by changing ambient conditions, such as moisture adsorption. Furthermore they found that deflection of metal-coated cantilevers is also thermally influenced (bimetallic effect). Later Thundat et al [69] observed changes in the resonance frequency of microcantilevers due to adsorption of analyte vapor on exposed surfaces. The frequency changes are caused through mass loading or adsorption-induced changes in cantilever spring constant. By coating cantilever surfaces with hygroscopic materials, such as phosphoric acid or gelatin, the cantilever can sense water vapor at picogram mass resolution.

9.1.2 Cantilever Sensors

Figure Lang_9.1

For the use of microcantilevers as sensors, neither a tip at the cantilever apex nor a sample surface is required. The microcantilever surfaces represent the platform to sense adsorption of molecules. Such processes involve generation of surface stress, resulting in bending of the microcantilever, provided adsorption preferentially occurs on one cantilever surface. Selective adsorption on one surface only is controlled by coating typically the upper surface with a thin layer showing affinity to the molecules in the environment to be detected. This surface will be called sensor surface or functionalized surface of the microcantilever (see Fig. 9.1a). The other surface, typically the lower surface, may be left uncoated or be coated with a passivation layer being inert or not exhibiting substantial affinity to the molecules that are to be detected. To establish functionalized surfaces, often a metal layer is evaporated onto the surface designed as sensor surface. Metal surfaces, such as gold, are frequently used to covalently bind a monolayer representing the actual detection layer, e.g. a thiol monolayer with defined surface chemistry. The molecules to be detected bind then to the thiol layer. The underlying gold coating also serves as reflection layer for optical readout of the cantilever.

Adsorption of molecules on the upper (functionalized) surface will produce a downward bending of the microcantilever due to formation of surface stress. This process is called formation of compressive surface stress (see Fig. 9.1b), because the adsorbed layer of molecules (e.g. a monolayer of alkylthiols) causes downward bending of the microcantilever away from its functionalized side. If the opposite situation occurs, i.e. when the microcantilever bends

upwards, tensile surface stress is produced (see Fig. 9.1c). A mixing of influences will take place, if both the upper and the lower surface of the microcantilever are prone to surface stress change effects. In this case, e.g. predominant compressive stress formation on the lower microcantilever surface might appear like tensile stress on the upper surface. Therefore, it is extremely important to properly passivate the lower surface so that no processes should take place on the lower surface of the microcantilever, facilitating evaluation and discussion of cantilever experiments.

9.1.3 Deflection measurement

Adsorption of molecules onto the functional layer causes stress formation at the interface between functional layer and the forming molecular layer, resulting in bending of the microcantilever, as the forces within the functional layer try to keep the distance between molecules constant. The cantilever beam bends due to its extreme flexibility. This property is reflected by the spring constant k of the cantilever. For a rectangular microcantilever of length l, thickness t and width w the spring constant is k is calculated as follows:

$$k = \frac{Ewt^3}{4l^3}, \tag{9.1}$$

where E is Young's modulus ($E_{Si} = 1.3 \times 10^{11}$ N/m^2 for Si(100)).
In first approximation the shape of the bent microcantilever is described as part of a circle with radius R. This radius of curvature is given by (Ibach [28]; Stoney [65])

$$\frac{1}{R} = \frac{6(1 \quad !)}{Et^2}, \tag{9.2}$$

The resulting surface stress change is described using Stoney's formula:

$$\Delta\sigma = \frac{Et^2}{6R(1-\nu)}, \tag{9.3}$$

where E is Young's modulus, t the thickness of the cantilever, ν the Poisson's ratio (ν_{Si} = 0.24), and R the bending radius of the cantilever.
The deflection of microcantilever sensors can be measured in various ways. They differ in sensitivity, effort for alignment and setup, robustness and ease of readout as well as in potential for miniaturization.

9.1.3.1 Piezoresistive Readout

Piezoresistive microcantilevers (Itoh et al [29]; Berger et al [4]) are usually U-shaped and have diffused piezoresistors in both of the legs near to the fixed end. The resistance in the piezoresistors is measured using a Wheatstone bridge circuit composed of three reference resistors, of which one is adjustable. The current flowing between the two branches of the Wheatstone bridge is first nulled by changing the resistance of the adjustable resistor. If the microcantilever bends, the piezoresistor changes its value and a current will flow between the two branches of the Wheatstone bridge. The current is converted via a differential amplifier into a voltage, which is proportional to the deflection value. For dynamic-mode measurement, the piezoresistive microcantilever is externally actuated via a piezocrystal driven by a frequency generator. The ac actuation voltage is fed as reference voltage into a lock-in amplifier and compared with the response of the Wheatstone bridge circuit allowing to sweep resonance curves and to determine shifts in resonance frequency.

9.1.3.2 Piezoelectric Readout

Piezoelectric microcantilevers (Lee et al [34]) are driven via the inverse piezoelectric effect (self-excitation) by applying an electric ac voltage to the piezoelectric material (lead zirconium titanate PZT or ZnO). Sensing of bending is performed by recording the piezoelectric current change taking advantage of the fact that the PZT layer produces a sensitive field response to weak stress through the direct piezoelectric effect. Piezoelectric microcantilevers are multilayer structures consisting of a SiO_2 cantilever and the PZT piezoelectric layer. Two electrode layers, insulated from each other, provide electrical contact. The entire structure is protected using passivation layers. An identical structure is usually integrated into the rigid chip body to provide a reference for the piezoelectric signals from the cantilever.

9.1.3.3 Capacitive Readout

Microcantilevers structures for capacitive readout are composed of a rigid beam with an electrode and a flexible cantilever with another electrode (Göddenhenrich et al [22]; Brugger et al [10]). Both electrodes are insulated from each other. When the flexible microcantilever is being bent, the capacitance between the two electrodes changes. From the capacitance change,

the cantilever deflection can be determined. Both measurement of static bending as well as determination of resonance frequency are possible.

9.1.3.4 Beam-Deflection Optical-Readout

Figure Lang_9.2

The most frequently used approach to read out microcantilever deflections is optical beam deflection (Meyer and Amer [40]), because it is a comparatively simple method, which has an excellent resolution.

The actual cantilever deflection Δx scales with the cantilever dimensions; therefore deflection responses should be expressed in terms of surface stress $\Delta\sigma$ in N/m to be able to compare cantilever responses acquired with different setups. Surface stress takes into account the cantilever material properties, such as Poisson ratio ν, Young's modulus E and the cantilever thickness t. The radius of curvature R of the cantilever characterizes bending, see Eq. (9.2). As shown in the drawing in Fig. 9.2, the actual cantilever displacement Δx is transformed into a displacement Δd on the position sensitive detector (PSD). The position of a light spot on a PSD is determined by measuring the photocurrents from the two facing electrodes. The movement of the light spot on the linear PSD is calculated from the two currents I_1 and I_2 and the size L of the PSD by

$$\Delta d = \frac{I_1 - I_2}{I_1 + I_2} \times \frac{L}{2}. \tag{9.4}$$

As all angles are very small, it can be assumed that the bending angle of the cantilever is equal to half of the angle θ of the deflected laser beam, i.e. $\theta/2$. Therefore, the bending angle of the cantilever can be calculated to be

$$\frac{\theta}{2} = \frac{\Delta d}{2s}\ , \tag{9.5}$$

where s is the distance between the PSD and the cantilever. The actual cantilever deflection Δx is calculated from the cantilever length l and the bending angle $\theta/2$ by

$$\Delta x = \frac{\theta/2}{2} \times l\,. \tag{9.6}$$

Combination of Eqs. (9.5) and (9.6) relates the actual cantilever deflection Δx to the PSD signal:

$$\Delta x = \frac{l \times \Delta d}{4s}. \tag{9.7}$$

The relation between the radius of curvature and the deflection angle is

$$\frac{\theta}{2} = \frac{l}{R}, \tag{9.8}$$

and after substitution becomes

$$R = \frac{2ls}{\Delta d} \quad \text{or} \quad R = \frac{2\Delta x}{l^2}. \tag{9.9}$$

9.2 Modes of operation

A microcantilever sensor is a versatile tool for investigation of various sample properties and allows to follow reactions occurring on its surface. Various operating modes have been presented.

Figure Lang_9.3

9.2.1 Static mode

Gradual bending of a microcantilever with molecular coverage is referred to as operation in the static mode (Fig. 9.3a). Various environments are possible, such as vacuum, ambient environment and liquids. In gaseous environment molecules adsorb on the functionalized sensing surface and form a molecular layer, provided there is affinity for the molecules to adhere to the surface. Polymer sensing layers show a partial sensitivity, because molecules from the environment diffuse into the polymer layer at different rates, mainly depending on the size and solubility of the molecules in the polymer layer. By selecting polymers among a wide range of hydrophilic/hydrophobic ligands, the chemical affinity of the surface can be influenced, because different polymers vary in diffusion suitability for polar/unpolar molecules. Thus, for detection in gas phase, the polymers can be chosen according to the detection problem, i.e. what the applications demand. Typical chemicals to be detected are

what the applications demand. Typical chemicals to be detected are volatile organic compounds (VOCs).

9.2.2 Dynamic mode

By oscillating a microcantilever at its eigenfrequency, information on the amount of molecules adsorbed can be obtained. However, the surface coverage is basically not known. Furthermore, molecules on the surface might be exchanged with molecules from the environment in a dynamic equilibrium.
In contrast, mass changes can be determined accurately by tracking the eigenfrequency of the microcantilever during mass adsorption or desorption. The eigenfrequency equals the resonance frequency of an oscillating microcantilever if its elastic properties remain unchanged during the molecule adsorption/desorption process and damping effects are negligible. This operation mode is called the dynamic mode (Fig. 9.3b) . The microcantilever is used as a microbalance, as with mass addition on the cantilever surface, the cantilever's eigenfrequency will shift to a lower value. The mass change on a rectangular cantilever is calculated (Thundat et al [68]) according to

$$\Delta m = (k/4\pi^2) \times (1/f_1^2 - 1/f_0^2) , \qquad (9.10)$$

where f_0 is the eigenfrequency before the mass change occurs, and f_1 the eigenfrequency after the mass change. For calculation of the spring constant k of the cantilever see Eq. (9.1).
Mass-change determination can be combined with varying environment temperature conditions to obtain a method introduced in the literature as "micromechanical thermogravimetry" (Berger et al [4]). The sample to be investigated has to be mounted at the apex of the cantilever. Its mass should not exceed several hundred nanograms. In case of adsorption, desorption or decomposition processes, mass changes in the picogram range can be observed in real time by tracking the resonance-frequency shift.

9.3 Functionalization

It is essential that the surfaces of the cantilever are coated in a proper way to provide suitable receptor surfaces for the molecules to be detected. Such coatings should be specific, homogeneous, stable, reproducible and either reusable or designed for single use only. For static mode measurements using the beam deflection technique, the cantilever's upper side, the sensor side, is coated with a 20 nm thick layer of gold as reflection layer. The coating method of choice should be fast, reproducible, reliable and allow one or both cantilever surfaces to be coated separately.

Figure Lang_9.4

For convenient coating with polymer layers, inkjet spotting is used, as it is possible to coat only the upper or lower surface. The method is also appropriate for coating many cantilever sensor arrays in a rapid and reliable way (Bietsch et al [5]; Bietsch et al [6]), see Fig. 9.4. An x-y-z positioning system allows a fine nozzle (capillary diameter: 70 µm) to be positioned with an accuracy of approx. 10 µm over a cantilever (Fig. 9.4a). Individual droplets (diameter: 60 – 80 µm, volume 0.1 – 0.3 nl) can be dispensed individually by means of a piezo-driven ejection system in the inkjet nozzle. When the droplets are spotted with a pitch smaller than 0.1 mm, they merge and form continuous films. By adjusting the number of droplets deposited on cantilevers, the resulting film thickness can be controlled precisely (Fig. 9.4b). The inkjet-spotting technique allows a cantilever to be coated within seconds and yields very homogeneous, reproducibly deposited layers of well-controlled thickness. Successful coating of self-assembled alkanethiol monolayers, polymer solutions, self-assembled DNA single-stranded oligonucleotides (Bietsch et al [6]) and protein layers has been demonstrated. This technique has been applied to functionalize a polymer coated microcantilever array for the chemical vapor detection experiments as described in the following section. In conclusion, inkjet spotting has turned out to be a very efficient and versatile method for functionalization that can even be used to coat arbitrarily-shaped sensors reproducibly and reliably (Lange et al [33]; Savran et al [60]).

9.4 Example of an optical beam-deflection setup

9.4.1 General description

A measurement setup for microcantilever arrays consists of four main parts: 1. the measurement chamber hosting the microcantilever array, 2. an optical or piezoresistive system to detect the cantilever deflection (e.g. laser sources, collimation lenses and a PSD, 3. electronics to amplify, process and acquire the signals from the PSD, and 4. a gas handling system to reproducibly inject samples into the measurement chamber and purge the chamber.

Figure Lang_9.5

Figure 9.5 shows a realization of a setup for experiments performed in gaseous environment. The microcantilever sensor array is hosted in an analysis chamber of 20 µl in volume, with inlet and outlet ports for gases. The bending of the microcantilevers is measured using an array of eight vertical-cavity surface-emitting lasers (VCSELs) arranged at a linear pitch of 250 µm that emit at a wavelength of 760 nm into a narrow cone of 5 to 10°.
The light of each VCSEL is collimated and focused onto the apex of the corresponding microcantilever by a pair of achromatic doublet lenses, 12.5 mm in diameter. This size was selected in order to make sure that all eight laser beams pass through the lenses close to its center in order to minimize scattering, chromatic and spherical aberration artifacts. The light is then reflected off the gold-coated surface of the cantilever and hits the surface of a PSD. As only a single PSD is used, the eight lasers cannot be switched on simultaneously. Therefore, a time-multiplexing procedure is used to switch the lasers on and off sequentially at typical intervals of 10-100 ms. The resulting deflection signal is digitized and stored together with time information on a personal computer (PC), which also controls the multiplexing of the VCSELs as well as the switching of the valves and mass flow controllers used for setting the composition ratio of the analyte mixture.

9.4.2 Cantilever-based electronic nose application

Besides specific receptor analyte binding, also the response pattern of a range of several differently coated sensors, e.g. coated with polymer layers, can be used to identify chemical vapors (artificial or electronic nose application). Using a cantilever array sensor setup consisting

of 8 polymer-coated cantilevers and automated gas handling system, several solvent vapors can be distinguished. 0.1 ml of various solvents was placed in vials, and the vapor from the headspace above the liquid was sampled using microcantilever sensors, operated in static deflection mode as a kind of artificial nose. Detection of vapors takes place via diffusion of the vapor molecules into the polymer, resulting in a swelling of the polymer and bending of the cantilever. Each cantilever is coated with a different polymer (see Fig. 9.6 and Table 9.1). The bending is specific for the interaction between solvent vapor and polymer time- and magnitude-wise.

Table 9.1

Figure Lang_9.6

Cantilever deflection traces upon subsequent injection of solvent vapor for 30s and purging with dry nitrogen for 150 s are shown in Fig. 9.7 for (a) water, (b) methanol and (c) ethanol. The cantilever deflections at 10, 20, 30 and 40 seconds after completion of solvent vapor injection are extracted. They describe the time-development of the curves in a reduced data set, i.e. 8 x 4 = 32 cantilever deflection amplitudes ('fingerprint') that account for a measurement data set. This data set is then evaluated using principal component analysis (PCA) techniques, extracting the most dominant deviations in the responses for the various sample vapors. The axes refer to projections of the multidimensional datasets into two dimensions (principal components). The labels in the PCA plot (Fig. 9.7d) indicate the individual measurements. The PCA plot shows well separated clusters of measurements indicating clear identification of vapor samples.

Figure Lang_9.7

5 Applications of cantilever based gas sensors

The application fields of microcantilever gas sensors are diverse: gas sensing, vapor sensing (artificial nose application), explosives detection, gas pressure and flow sensing. The follow-

ing sections will review some recent publications in these fields, complemented by theory, simulation and fabrication aspects.

9.5.1 Gas sensing

Several publications investigate the detection of hydrogen using Pd-coated cantilever sensors. Hu et al [27] have studied bulk adsorption of hydrogen on palladium using differential stress formation on a bimaterial cantilever. The adsorption of hydrogen into palladium results in film expansion, whereby the bending magnitude is proportional to hydrogen partial pressure. Bending also depends on the thickness of the Pd film and is reversible. Unlike hydrogen adsorption, mercury adsorption on a gold film is irreversible, as it is a surface adsorption process. Baselt et al [3] describe the design of a microelectromechanical (MEMS) hydrogen sensor consisting of an array of 10 micromachined cantilever beams. The deflection is measured using the capacitive method with a dedicated readout circuit including wireless transmitters capable of transmitting data over a distance of 30m. The sensitive coating is composed of 90% Pd and 10% Ni and can easily detect concentrations of 0.4 % hydrogen. It operates reversibly. Influences of relative humidity and temperature have also been studied. Fabre et al [18] present a hydrogen sensor based on Pd-coated microcantilevers. It was found that the surface stress response depends strongly on the hydrogen dissociation into the bulk of the Pd layer, whereby the influences of cantilever shape and surface roughness play also an important role. Ono et al [44] report resonating cantilever sensors to investigate the hydrogen storage capacity of carbon nanotubes (CNT). The storage capacity was found to be up to 6% and the mass resolution was on the order of attogram. Zhou et al [76] use self-excited piezoelectric microcantilevers with a layer of MFI zeolites to detect Freon down to a concentration of 10 ppm, whereby ethanol vapor shows no effect up to the largest concentration of 500 ppm that was measured (Zhou et al [77]).

Mertens et al [38] presented results on detection of HF, a decomposition product of nerve gas agents, using SiO_2 coated Si_3N_4 microcantilevers. Detection based on etching of SiO_2 was achieved in the range from 0.26 to 13 ppm. Embedded piezoresistive cantilevers have been used by Kooser et al [32] for detection of carbon monoxide using a nickel-containing polyethylene oxide (PEO) layer for detection. Ni has been added to the PEO solution as nickel acetate and serves for resistivity measurement. After drying for 24 h and exposure for 1 h to dry nitrogen, the sensor was exposed to carbon monoxide, resulting in a resistance drop. For concentration ratios up to 1:10 ($CO:N_2$) the sensor response was fully reversible. Adams et al [1]

report on piezoelectric cantilevers for mercury detection down to a concentration of 50 ppb. Again, after three subsequent exposure steps, the cantilever was irreversibly saturated. Porter et al [57] demonstrate HCN detection using embedded piezoresistive microcantilever sensors down to a concentration of 150 ppm. HCN was generated by reacting KCN with sulfuric acid. No response was observed for H_2SO_4 vapors only. Sensitivities are summarized in Table 9.2

Table 9.2

9.5.2 Chemical vapor detection

Jensenius et al [30] describe a microcantilever-based alcohol vapor sensor using the piezoresistive technique and polymer coating. They also present a simple evaporation model that allows determining the concentration. The detection limit found amounts to 10 ppm for methanol, ethanol and 2-propanol. Hierlemann et al [26] present an integrated complementary metal oxide semiconductor (CMOS) chemical microsensor with piezoresistive detection (Wheatstone bridge configuration) using poly(etherurethane) (PEUT) as the sensor layer. They are able to reversibly detect volatile organic compounds (VOCs) such as toluene, n-octane, ethyl acetate and ethanol with a sensitivity level down to 200 ppm. An improved version of that device is described by Lange et al [33]. The sensitivity could be increased to 5 ppm for n-octane. Later the technique has been refined by using electromagnetic rather than electrothermal actuation and transistor-based readout reducing power dissipation on the cantilever [70]. Fadel et al [19] describe piezoelectric readout in dynamic mode and electromagnetic actuation of cantilevers spray-coated with PEUT, achieving a sensitivity of 14 ppm for ethanol. Wright et al [75] published a study how to prepare polyethylene glycol (PEG) coated microcantilever sensors using a microcapillary pipette assisted method. PEG coating is suitable for ethanol sensing as ethanol quickly forms hydrogen bonds with the OH groups of the PEG. Sensor operation is reported to be reversible and reproducible. Senesac et al [61] use artificial neural networks for analyte species and concentration identification with polymer coated optically read-out microcantilevers. The analytes detected are carbon dioxide, dichloromethane, diisopropylmethylphosphonate (DIMP), dioxane, ethanol, water, 2-propanol, methanol, trichloroethylene and trichloromethylene. Lochon et al [36] investigate the chemical sensing performance of a silicon reconant microcantilever sensor in dependence on the thickness of the sensitive coating. For a coating thickness of 1, 4 and 21 micrometers of PEUT a limit of detection of 30 ppm was found for ethanol. Satyanarayana et al [59] present a new concept of

parylene micro membrane array for chemical sensing using the capacitive method. The parylene membrane is suspended over a metal pad patterned on the substrate. The pad and part of the membrane that is metal-coated serves as electrodes for capacitive measurement. The top electrode located on the membrane is chemically modified by applying a gold layer and self-assembled thiol monolayers (-COOH, -CH_3 and –OH) for detection of analyte molecules. Successful detection of 2-propanol and toluene is reported. Then et al [67] describe a sensitive self-oscillating cantilever array for quantitative and qualitative analysis of organic vapor mixtures. The cantilevers are electromagnetically actuated and the resonance frequency is measured using a frequency counter. Sensor response is reproducible and reversible. Using PEUT coating the smallest measured concentration is 400 ppm, but the limit of detection is well below 1 ppm. Chapman et al [11] report on a combination of gas chromatography with a microcantilever sensor array for enhanced selectivity. Test VOC mixtures composed of acetone, ethanol and trichloroethylene in pentane, as well as methanol with acetonitrile in pentane were first separated in a gas chromatography column and then detected using micocantilevers coated with responsive phases such as 3-aminopropyltriethoxy silane, copper phtalocyanine and methyl-β-cyclodextrin. Analytes detected include pentane, methanol, acetonitrile, acetone, ethanol and trichloroethylene. Archibald et al [2] present results on independent component analysis (ICA) of ethanol, propanol and DIMP using cantilever coated with molecular recognition phases (MRP), whereby ICA has proven its feature extraction ablility for components in mixtures. Sensitivities are summarized in Table 9.3

Table 9.3

9.5.3 Explosives detection

Preventive counter measures against terrorism threats require inexpensive, highly selective and very sensitive small sensors that can be mass-produced and micro-fabricated. Such low cost sensors could be arranged as a sensor grid for large area coverage of sensitive infrastructure, like airports, public buildings, or traffic infrastructure. Threats can be of chemical, biological, radioactive or explosive nature. Microfabricated detectors for explosives might be very useful for passenger baggage-screening, as compact versions of established technologies like the ion mobility spectrometer [17] or nuclear quadrupole resonance [20] have been developed, but are not likely to be miniaturized further. Another application area would be detection of landmines.

Microcantilever sensors offer sensitivities more than two orders of magnitude better than quartz crystal microbalances [43], flexural plate wave oscillators [15] and surface acoustic wave devices [23]. Several approaches to detect dangerous chemicals are already described in literature: photomechanical chemical microsensors based on adsorption-induced and photo-induced stress changes due to the presence of diisopropyl methyl phosphonate (DIMP), which is a model compound for phosphorous-containing chemical warfare agents, and trinitrotoluene (TNT), an explosive [16]. Further explosives frequently used include pentaerythritol tetranitrate (PETN) and hexahydro-1,3,5-triazine (RDX), often also with plastic fillers [49]. These compounds are very stable, if no detonator is present. Their explosive power, however, is very large, and moreover, the vapor pressures of PETN and RDX are very low, in the range of ppb and ppt. By functionalizing microcantilevers with self-assembled monolayers of 4-mercaptobeonzoic acid (4-MBA) PETN was detected at a level of 1400 ppt and RDX at a level of 290 ppt [50]. TNT was found to readily stick to Si surfaces, suggesting the use of microcantilevers for TNT detection, taking advantage of the respective adsorption/desorption kinetics [51,52]. Detection of TNT via deflagration on a microcantilever is described by Pinnaduwage et al [52]. They used piezoresistive microcantilevers where the cantilever deflection was measured optically via beam deflection. TNT vapor from a generator placed 5 mm away from the microcantilever was observed to adsorb on its surface resulting in a decrease of resonance frequency. Application of an electrical pulse (10 V, 10 ms) to the piezoresistive cantilever resulted in deflagration of the TNT vapor and a bump in the cantilever bending signal. This bump was found to be related to the heat produced during deflagration. The amount of heat released is proportional to the area of the bump in the time vs. bending signal diagram of the process. The deflagration was found to be complete, as the same resonance frequency as before the experiment was observed. The amount of TNT mass involved was determined as 50 pg. The technique was later extended to the detection of PETN and RDX, where much slower reaction kinetics was observed [50,53]. Traces of 2,4-dinitrotoluene (DNT) in TNT can also be used for detection of TNT, because it is the major impurity in production grade TNT. Furthermore DNT is a decomposition product of TNT. The saturation concentration of DNT in air at 20°C is 25 times higher than that of TNT. DNT was reported detectable at the 300 ppt level using polysiloxane polymer layers [54]. Microfabrication of electrostatically actuated resonant microcantilever beams in CMOS technology for detection of the nerve agent stimulant dimethylmethylphosphonate (DMMP) using polycarbosilane-coated beams [71] is an important step towards an integrated platform based on silicon microcantilevers, which besides compactness might also include telemetry [55]. Sensitivities are summarized in Table 9.4

Table 9.4

9.5.4 Gas pressure and flow sensing

Gas sensing does not only involve chemical detection, but also pressure and flow sensing. Brown et al [8] have studied the behavior of magnetically actuated oscillating microcantilevers at large deflections and have found hysteresis behavior at resonance. The amplitude at the actuation frequency changes depending on pressure due to damping. The authors have used cantilever in cantilever (CIC) structures, and have observed changes in deflection as gas pressure is varied. At atmospheric pressure, damping is large and the oscillation amplitude is relative small and hysteresis effects are absent. At lower pressure, abrupt changes in the oscillation amplitude occur with changes in the driving frequency. Since the change of amplitude and driving frequency, at which they occur are pressure dependent, these quantities can be used for accurate determination of gas pressure, demonstrated in the range between 10^{-3} and 10^{2} Torr. Brown et al [9] emphasize that microelectromechanical system pressure sensors will have a wide range of applications, especially in the automotive industry. Piezoresistive cantilever based deflection measurement has major advantages over diaphragms. The pressure range has been extended to 15-1450 Torr by means of design geometry adaptation. Su et al [66] present highly sensitive ultra-thin piezoresistive silicon microcantilevers for gas velocity sensing, whereby the deflection increases with airflow distribution in a steel pipe. The detection principle is based on normal pressure drag producing bending of the cantilever. The minimum flow speed measured was 7.0 cm/s, which is comparable to classical hot-wire anemometers. Mertens et al [39] have investigated the effects of temperature and pressure on microcantilever resonance response in helium and nitrogen. Resonance response as a function of pressure showed three different regimes, which correspond to molecular flow, transition regimes and viscous flow, whereby the frequency variation of the cantilever is mainly due to changes in the mean free path of gas molecules. Effects observed allow measurement of pressures between 10^{-2} and 10^{6} Pa. Mortet et al [41] present a pressure sensor based on a piezoelectric bimorph microcantilever with a measurement range between 0.1 and 8.5 bar. The resonance frequency shift is constant for pressures below 0.5 bar. For higher pressures the sensitivity is typically a few ppm/mbar, but depends on the mode number. Sievilä et al [63] present a cantilever paddle within a frame operating like a moving mirror to detect the displacements in the oscillating cantilever using a He/Ne laser in a Michelson interferometer

configuration, whereby the cantilever acts as moving mirror element in one path of the interferometer. A fixed mirror serves a reference in the other arm of the interferometer. Sensitivities are summarized in Table 9.5

Table 9.5

9.6 Other techniques

9.6.1 Metal Oxide Gas Sensors

Tin dioxide is the most investigated material for metal-oxide based gas sensors, capable for detection of a wide range of gases [12]. The technique takes advantage of the fact that the resistance of the semiconductor changes with the ambient gas concentration and therefore the rate of redox reactions is measured. Sensor elements are typically operated at temperatures between 300 and 550 °C. The sintered polycrystalline surface is responsible for a large resistance change, oxygen absorption increases the potential barrier between grain boundaries. By doping of SnO_2 with silicon the selectivity can be enhanced [14]. Doping of SnO_2 with 0.1 wt % of Ca and Pt allows detecting various volatile organic compounds [35]. Sputtered WO_3 thin films containing Pd, Au, Bi or Sb catalyst have been recognized as promising candidates for sensing elements in gas analysis [45]. Sensitivities are summarized in Table 9.6

Table 9.6

9.6.2 Quartz Crystal Microbalance

Quartz crystal microbalance (QMB) sensors (see also Chapter 8) are based on a piezoelectric substrate (quartz). When actuated by an alternating field, elastic waves are generated in the quartz crystal (typically at 10 MHz). Temporarily absorbed molecules perturb the propagation of acoustic waves because of the added mass (microbalance) and by changing the viscoelastic properties. From the shift of the fundamental frequency, the adsorbed mass can be measured at ppm sensitivity [24]. Specific realizations of resonance based sensors are surface acoustic sensors (SAW), thickness-shear mode sensors (TSM) and flexural plate wave (FPW) devices.

9.6.3 Conducting Polymer Sensors

Conducting polymer sensors are based on chemoresistors (see also Chapter 5) that are manufactured by dissolving a chemically sensitive polymer in an appropriate solvent and mixing the dissolved polymer with conductive carbon particles [62]. This mixture (ink) is then deposited and dried onto a solid substrate on which a metal electrode has been applied previously. The upper surface of the polymer layer is also coated partially with a metal electrode. When chemical vapors come into contact with the polymers, the vapor will diffuse into the polymer layer, producing swelling of the polymer. The swelling changes the resistance between the electrodes, and a response signal can be measured and recorded. The amount of swelling is proportional to the concentration of the vapor present. A variety of volatile organic compounds can be detected in this way. By purging with e.g. dry nitrogen gas the swelling process can be reversed. For trichloroethylene concentrations between 1'000 and 10'000 ppm have been detected with polyisobutylene or polyepichlorohydrine modified with carbon black [58]. Using poly-N-vinyl-pyrrolidone and carbon black, methanol and ethanol have been detected at the ppt level [37]. A different possibility to apply conductive polymers for detection of volatile organic compounds is the use of piezoresistive microcantilevers embedded in conducting polymers [56]. This design has the advantage of higher stability and ease of use, since only an ohmmeter connected to the piezoresistors is required for measurements.

9.6.4 Surface acoustic waves

The principle of using the surface acoustic wave (SAW) effect for chemical vapor sensing is pioneered by Wohltjen and Dessy [73] and described in detail by Wohltjen [74] (see also Chapter 8). SAW devices are frequently used for chemical vapor detection because of the ruggedness, low cost, electronic output, sensitivity and adaptibility to a wider variety of vapors. The substrate for a SAW device must be piezoelectric (e.g. quartz) to permit the easy generation of radio frequency Rayleigh waves. As chemical sensor often a polymer layer is applied. The resonance frequency of the device is measured during exposure to the analyte vapor, allowing to deduce the mass change caused by the adsorbing vapor molecules. Using SAW multisensors and pattern recognition techniques vapors can be detected routinely in the ppm range [46,47], see Table 9.7

Table 9.7

9.6.5 Field effect transistor sensors devices

The detection principle of field effect transistor (FET) sensors with catalytic metal gates is based on the change of the electric field in the insulator, into which gases diffuse (see also Chapter 4). Therewith the number of mobile carriers in the semiconductor is changed. Spetz et al [64] use SiC FET sensors to monitor combustion processes at temperatures up to 1000 °C. By use of different gate electrode materials the selectivity towards specific gases can be optimized, as well as by choice of the operation temperature. Measured concentrations range from a few ten ppm to 12 %, as seen from Table 9.8

Table 9.8

Acknowledgments

I thank R. McKendry (University College London, London, U.K.), M. Hegner, W. Grange, Th. Braun (CRANN Dublin), Ch. Gerber, J. Zhang, A. Bietsch, V. Barwich, M. Ghatkesar, F. Huber, N. Backmann, G. Yoshikawa, J.-P. Ramseyer, A. Tonin, H.R. Hidber, E. Meyer and H.-J. Güntherodt (University of Basel, Basel, Switzerland) for valuable contributions and discussions, as well as U. Drechsler, M. Despont, H. Schmid, E. Delamarche, H. Wolf, R. Stutz, R. Allenspach, and P.F. Seidler (IBM Research, Zurich Research Laboratory, Rüschlikon, Switzerland). I also thank the European Union FP 6 Network of Excellence FRONTIERS for support. This project is funded partially by the National Center of Competence in Research in Nanoscience (Basel, Switzerland), the Swiss National Science Foundation and the Commission for Technology and Innovation (Bern, Switzerland).

References

[1] Adams JD, Rogers B, Manning L, Hu Z, Thundat T, Cavazos H, Minne SC (2005) Piezoelectric self-sensing of adsorption-induced microcantilever bending. Sens Act A 121: 457-461

[2] Archibald R, Datskos P, Devault G, Lamberti V, Lavrik N, Noid D, Sepianiak M, Dutta P (2007) Independent component analysis of Nanomechanical responses of cantilever arrays. Anal Chim Acta 584:101-105

[3] Balselt DR, Fruhberger B, Klassen E, Cemalovic S, Britton Jr CL, Patel SV, Mlsna TE, McCorkle D, Warmack B (2003) Design and performance of a microcantilever-based hydrogen sensor. Sens Act B 88:120-131

[4] Berger R, Lang HP, Gerber C, Gimzewski JK, Fabian JH, Scandella L, Meyer E, Güntherodt HJ (1998) Micromechanical thermogravimetry. Chem Phys Lett 294:363

[5] Bietsch A, Hegner M, Lang HP, Gerber C (2004) Inkjet deposition of alkanethiolate monolayers and DNA oligonucleotides on gold: Evaluation of spot uniformity by wet etching. Langmuir 20:5119-5122

[6] Bietsch A, Zhang J, Hegner M, Lang HP, Gerber C (2004) Rapid functionalization of cantilever array sensors by inkjet printing. Nanotechnology 15:873-880

[7] Binnig G, Quate CF, Gerber C (1986) Atomic force microscope. Phys Rev Lett 56:930-933

[8] Brown KB, Ma Y, Allegretto W, Lawson RPW, Vermeulen FE, Robinson AM (2001) Microstructural pressure sensor based on an enhanced resonant mode hysteresis effect. J Vac Sci Technol B 19:1628-1632

[9] Brown KB, Allegretto W, Vermeulen FE, Robinson AM (2002) Simple resonating microstructures for gas pressure measurement. J Micromech Microeng 12:204-210

[10] Brugger J, Buser RA, de Rooij NF (1992) Micromachined atomic force microprobe with integrated capacitive read-out. J Micromech Microeng 2:218-220

[11] Chapman PJ, Vogt F, Dutta P, Datskos PG, Devault GL, Sepianiak MJ (2007) Facile hyphenation of gas chromatography and a microcantilever array sensor for enhanced selectivity. Anal Chem 79:364-370

[12] Chiorino A, Ghiotti G, Prinetto F, Carotta MC, Gnani D, Martinelli G (1999) Preparation, characterization of SnO_2, MoO_x-SnO_2 nano-sized powders for thick film gas sensors. Sens Act B 58:338-349

[13] Cleveland JP, Manne S, Bocek D, Hansma PK (1993) A Nondestructive Method for Determining the Spring Constant of Cantilevers for Scanning Force Microscopy. Rev Sci Instrum 64:403-405

[14] Comini, E, Faglia G, Sberveglieri G (2001) CO and NO_2 response of tin oxide silicon doped thin films. Sens Act B 76:270-274

[15] Cunningham B, Weinberg M, Pepper J, Clapp C, Bousquet R, Hugh B, Kant R, Daly C, Hauser E (2001) Design, fabrication and vapor characterization of a microfabricated flexural plate resonator sensor and application to integrated sensor arrays. Sens Actuators B 73:112-123

[16] Datskos PG, Sepaniak MJ, Tipple CA, Lavrik N (2001) Photomechanical chemical microsensors. Sens. Act. B 76:393-402

[17] Ewing RG, Miller CJ (2001) Detection of volatile vapors emitted from explosives with a handheld ion mobility spectrometer. Field Anal. Chem. Technol. 5:215-221

[18] Fabre A, Finot E, Demoment J, Contreras S (2002) Monitoring the chemical changes in Pd induced by hydrogen absorption using microcantilevers. Ultramicroscopy 97:425-432

[19] Fadel L, Lochon F, Dufour I, Français (2004) Chemical sensing: millimeter size resonant microcantilever performance. J Mcromech Microeng 14 :S23-S30

[20] Garroway AN, Buess ML, Miller JB, Suits BH, Hibbs AD, Barrall GA, Matthews R, Burnett LJ (2001) Remote sensing by nuclear quadrupole resonance. IEEE Trans. Geosci. Remote Sens 39:1108-1118

[21] Gimzewski JK, Gerber C, Meyer E, Schlittler RR (1994) Observation of a Chemical-Reaction Using a Micromechanical Sensor. Chem Phys Lett 217:589-594

[22] Göddenhenrich T, Lemke H, Hartmann U, Heiden C (1990) Force Microscope with capacitive displacement detection. J Vac Sci Technol A 8:383-387

[23] Grate JW (2000) Acoustic wave microsensor arrays for vapor sensing. Chem. Rev. (Washington, D.C.) 100:2627-2647

[24] Guan S (2003) Frequency encoding of resonant mass sensors for chemical vapor detection. Anal Chem 75:4551-4557

[25] Heng TMS (1971) Trimming of Microstrip Circuits Utilizing Microcantilever Air Gaps. IEEE Trans Microwave Theory and Techn 19:652-654

[26] Hierlemann A, Lange D, Hagleitner C, Kerness N, Koll A, Brand O, Baltes H (2000) Application-specific sensor systems based on CMOS chemical microsensors. Sens Act B 70:2-11

[27] Hu Z, Thundat T, Warmack RJ (2001) Investigation of adsorption and adsorption-induced stresses using microcantilever sensors. J Appl Phys 90:427-431

[28] Ibach H (1994) Adsorbate-Induced Surface Stress. J Vac Sci Technol A 12:2240-2243

[29] Itoh T, Suga T (1994) Force Sensing Microcantilevers using Sputtered Zinc-Oxide Thin-Film. Appl Phys Lett 64:37-39

[30] Jensenius H, Thaysen J, Rasmussen AA, Veje LH, Hansen O, Boisen A (2000) A microcantilever-based alcohol vapor sensor-application and response model. Appl Phys Lett 76:2815-2817

[31] Kolesar ES (1983) United States Patent No. 4,549,427, filed Sept 19, 1983

[32] Kooser A, Gunter RL, Delinger WD, Porter TL, Eastman MP (2004) Gas sensing using embedded piezoresistive microcantilever sensors. Sens Act B 99:474-479

[33] Lange D, Hagleitner C, Hierlemann A, Brand O, Baltes H (2002) Complementary Metal Oxide Semiconductor Cantilever Arrays on a Single Chip: Mass-Sensitive Detection of Volatile Organic Compounds. Anal Chem 74:3084-3095

[34] Lee C, Itoh T, Ohashi T, Maeda R, Suga T (1997) Development of a piezoelectric self-excitation and self-detection mechanism in PZT microcantilevers for dynamic scanning force microscopy in liquid. J Vac Sci Technol B 15:1559-1563

[35] Lee DS, Jung JK, Lim JW, Huh JS, Lee DD (2001) Recognition of volatile organic compounds using SnO_2 sensor array and pattern recognition analysis. Sens Act B 77:228-236

[36] Lochon F, Fadel L, Dufour I, Rebière D, Pistré J (2006) Silicon made resonant microcantilever: Dependence of the chemical sensing performances on the sensitive coating thickness. Mat Sci Eng C 26:348-353

[37] Longeran MC, Severin EJ, Doleman BJ, Beaber SA, Grubbs RH, Lewis NS (1996) Array-Based Vapor Sensing Using Chemically Sensitive, Carbon Black-Polymer Resistors. Chem Mater 8:2298-2312

[38] Mertens J, Finot E, Nadal MH, Eyraud V, Heintz O, Bourillot E (2003) Detection of gas trace of hydrofluoric acid using microcantilever. Sens Act B 99:58-65

[39] Mertens J, Finot E, Thundat T, Fabre A, Nadal MH, Eyraud V, Bourillot E (2003) Effects of temperature and pressure on microcantilever resonance response. Ultramicroscopy 97:119-126

[40] Meyer G, Amer NM (1988) Novel optical approach to atomic force microscopy. Appl Phys Lett 53:2400-2402

[41] Mortet V, Petersen R, Haenen K, D'Olieslaeger M (2006) Wide range pressure sensor based on a piezoelectric bimorph microcantilever. Appl Phys Lett 88:133511

[42] Muralidharan G, Wig A, Pinnaduwage LA, Hedden D, Thundat T, Lareau RT (2003) Absorption-desorption characteristics of explosive vapors investigated with microcantilevers. Ultramicroscopy 97:433-439

[43] O'Sullivan CK, Guilbault GG (1999) Commercial quartz crystal microbalances – theory and applications. Biosens Bioelectron 14:663-670

[44] Ono T, Li X, Miyashita H, Esashi M (2003) Mass sensing of adsorbed molecules in sub-picogram sample with ultrathin silicon resonator. Rev Sci Instrum 74:1240-1243

[45] Penza M, Cassano G, Tortorella F (2001) Gas recognition by activated WO3 thin-film sensors array. Sens Act B 81:115-121

[46] Penza M, Cassano G, Tortorella F (2002) Identification and quantification of individual volatile organic compounds in a binary mixture by SAW multisensor array and pattern recognition analysis. Meas Sci Technol 13:846-858

[47] Penza M, Cassano G (2003) Application of principal component analysis and artificial neural networks to recognize the individual VOCs of methanol/2-propanol in a binary mixture by SAW multi-sensor array. Sens Act B 89:269-284

[48] Petersen KE (1979) Micromechanical Membrane Switches on Silicon. IBM J Res Develop 23:376-385

[49] Pinnaduwage LA, Boiadjiev V, Hawk JE, Thundat T (2003) Sensitive detection of plastic explosives with self-assembled monolayer-coated microcantilevers. Appl Phys Lett 83:1471-1473

[50] Pinnaduwage LA, Gehl A, Hedden DL, Muralidharan G, Thundat T, Lareau RT, Sulchek T, Manning L, Rogers B, Jones M, Adams JD (2003) A microsensor for trinitrotoluene vapour. Nature 425:474-474

[51] Pinnaduwage LA, Yi D, Tian F, Thundat T, Lareau RT (2004) Adsorption of trinitrotoluene on uncoated silicon microcantilever surfaces Langmuir 20:2690-2694.

[52] Pinnaduwage LA, Wig A, Hedden DL, Gehl A, Yi D, Thundat T, Lareau RT (2004) Detection of trinitrotoluene via deflagration on a microcantilever. J Appl Phys 95:5871-5875

[53] Pinnaduwage LA, Thundat T, Gehl A, Wilson SD, Hedden DL, Lareau RT (2004) Desorption characteristics, of uncoated silicon microcantilever surfaces for explosive and common nonexplosive vapors. Ultramicroscopy 100:211-216

[54] Pinnaduwage LA, Thundat T, Hawk JE, Hedden DL, Britt R, Houser EJ, Stepnowski S, McGill RA, Bubb D (2004) Detection of 2,4-dinitrotoluene using microcantilever sensors. Sens Act B 99:223-229

[55] Pinnaduwage LA, Ji HF, Thundat T (2005) Moore's law in homeland defense: An integrated sensor platform based on silicon microcantilevers. IEEE Sensors J 5:774-785

[56] Porter TL, Eastman MP, Macomber C, Delinger WG, Zhine R (2003) An embedded polymer piezoresistive microcantilever sensor. Ultramicroscopy 97:365-369

[57] Porter TL, Vail TL, Eastman MP, Stewart R, Reed J, Venedam R, Delinger W (2007) A solid-state sensor platform for the detection of hydrogen cyanide gas. Sens Act B 123:313-317

[58] Rivera D, Alam MK, Davis CE, Ho, CK (2003) Characterization of the ability of polymeric chemiresistor arrays to quantitate trichloroethylene using partial least squares (PLS): effects of experimental design, humidity, and temperature. Sens Act B 92:110-120

[59] Satyanarayana S, McCormick DT, Majumdar A (2006) Parylene micro membrane capacitive sensor array for chemical and biological sensing. Sens Act B 115:494-502

[60] Savran CA, Burg TP, Fritz J, Manalis SR (2003) Microfabricated mechanical biosensor with inherently differential readout. Appl Phys Lett 83:1659-1661

[61] Senesac LR, Dutta P, Datskos PG, Sepianiak MJ (2006) Analyte species and concentration identification using differentially functionalized microcantilever arrays and artificial neural networks. Anal Chim Acta 558:94-101

[62] Severin EJ, Lewis, NS (2000) Relationships among Resonant Frequency Changes on a Coated Quartz Crystal Microbalance, Thickness Changes, and Resistance Responses of Polymer-Carbon Black Composite Chemiresistors. Anal Chem 72:2008-2015

[63] Sievilä P, Rytkönen VP, Hahtela O, Chekurov N, Kauppinen J, Tittonen I (2007) Fabrication and characterization of an ultrasensitive acousto-optical cantilever. J Micromech Microeng 17:852-859

[64] Spetz AL, Tobias P, Uneus L, Svenningstorp H, Ekedahl LG, Lundstrom I (2000) High temperature catalytic metal field effect transistors for industrial applications. Sens Act B 70:67-76

[65] Stoney GG (1909) The tension of thin metallic films deposited by electrolysis. Proc R Soc London Ser A 82:172-175

[66] Su Y, Evans AGR, Brunnschweiler A, Ensell G (2002) Characterization of a highly sensitive ultra-thin piezoresistive silicon cantilever probe and its application in gas flow velocity sensing. J Micromech Microeng 12:780-785

[67] Then D, Vidic A, Ziegler C (2006) A highly sensitive self-oscillating cantilever array for the quantitative and qualitative analysis of organic vapor mixtures. Sens Act B 117:1-9

[68] Thundat T, Warmack RJ, Chen GY, Allison DP (1994) Thermal and Ambient-Induced Deflections of Scanning Force Microscope Cantilevers. Appl Phys Lett 64:2894-2896

[69] Thundat T, Chen GY, Warmack RJ, Allison DP, Wachter EA (1995) Vapor Detection Using Resonating Microcantilevers. Anal Chem 67:519-521

[70] Vancura C, Rüegg M, Li Y, Hagleitner C, Hierlemann A (2005) Magneticallz Actuated Complementarz Metal Oxide Semiconductor Resonant Cantilever Gas Sensor Systems. Anal Chem 77:2690-2699

[71] Voiculescu I, Zaghloul ME, McGill RA, Houser EJ, Fedder GK (2005) Electrostatically actuated resonant microcantilever beam in CMOS technology for the detection of chemical weapons. IEEE Sensors J. 5:641-647

[72] Wilfinger RJ, Bardell PH, Chhabra DS (1968) Resonistor – A frequency selective device utilizing mechanical resonance of a silicon substrate, IBM J Res Develop 12:113-118

[73] Wohltjen, H, Dessy RE (1979) Surface acoustic probe for chemical analysis I. Introduction and instrument description. Anal Chem 51:1458-1475

[74] Wohltjen, H (1984) Mechanism of operation and design considerations for surface acoustic wave device vapour sensors. Sens Act 5:307-325

[75] Wright YJ, Kar AK, Kim YW, Scholz C, George MA (2005) Study of microcapillary pipette-assisted method to prepare polyethylene glycol-coated microcantilever sensors. Sens Act B 107:242-251

[76] Zhou J, Li P, Zhang S, Huang Y, Yang P, Bao M, Ruan G (2003) Self excited piezoelectric microcantilever for gas detection. Microelectr Eng 69:37-46

[77] Zhou J, Li P, Zhang S, Long Y, Zhou F, Huang Y, Yang P, Bao M (2003) Zeolite-modifies microcantilever gas sensor for indoor air quality control. Sens Act B 94:337-342

Figure Legends

Figure 9.1: (a) Schematic drawing of a microcantilever with its lower surface passivated and it upper surface functionalized for recognition of target molecules, (b) downward bending of a microcantilever due to compressive surface stress, (c) upward bending due to tensile surface stress.

Figure 9.2: Beam-deflection concept to determine microcantilever bending with an accuracy of one nanometer.

Figure 9.3: Major operating modes of microcantilever sensors: (a) static mode exploiting surface stress changes, (b) dynamic mode to extract mass changes.

Figure 9.4: (a) Schematic drawing of single-sided microcantilever coating using an inkjet spotter. (b) Optical micrograph of the inkjet spotter nozzle. The amount of liquid containing the probe molecules can be dosed accurately by choosing the number of drops being ejected from the nozzle.

Figure 9.5: (a) Realization of a static mode beam-deflection microcantilever-array sensor setup for measurements in gas. A HPLC 6-way valve is used to select vapor from the headspace of a vial filled with liquid sample. The vapor is transported by nitrogen carrier gas to the measurement chamber hosting the microcantilever array. The microcantilever bending is measured using optical beam deflection involving VCSELs and a PSD. The location of the laser spot indicating microcantilever bending is processed and digitized using measurement electronics and a data acquisition card in a personal computer. (b) Gas handling system consisting of mass flow controllers and syringe pumps for well-defined flow rates.

Figure 9.6: Optical microscopy image of a polymer-coated microcantilever array for application as an artificial nose for solvents. The pitch between microcantilevers is 250 micron.

Figure 9.7: Application of microcantilever array sensors as artificial electronic nose. Measurement traces of microcantilevers coated with polymers during the detection of (a) water, (b) methanol, (c) ethanol. For every solvent, four consecutive injections of vapor saturated with solvent are shown. Upon injection of solvent vapor, the microcantilevers deflect in a specific way due to the swelling of the polymers layer on exposure to the solvent vapor. Subsequent

purging of the measurement chamber with dry nitrogen gas (flow rate: 100 ml/min.) promotes diffusion of the solvent molecules out of the polymer layer, resulting in bending back of the microcantilevers to the baseline. (d) Principal component analysis (PCA) of the response patterns of all eight microcantilevers upon exposure to the three different solvent vapors. Clear separation of the clusters proves the excellent distinction capability of the artificial nose setup. Each symbol in the PCA plot corresponds to one of the injections in (a)-(c).

Tables

Table 9.1 Polymer coatings

Cantilever	Polymer	Full name of compound
1	PSS	Poly(sodium 4-styrenesulfonate)
2	PEI	Polyethylenimine
3	PAAM	Poly(allylamine hydrochloride)
4	CMC	Carboxymethylcellulose sodium salt
5	Dextran	Dextran from Leuconostoc spp.
6	HPC	Hydroxypropyl cellulose
7	PVP	Polyvinylpyrrolidone
8	PEO	Poly(2-ethyl-2-oxazoline)

Table 9.2 Detection limits of gaseous analytes

Analyte	Detection limit	Reference
H_2	20 ppm	Hu et al [27]
Hg	0.4 ppb	Hu et al [27]
Hg	50 ppb	Adams et al [1]
Hg	4000 ppm	Baselt et al [3]
Freon	10 ppm	Zhou et al [76]
HF	0.26 ppm	Mertens et al [38]
HCN	150 ppm	Porter et al [57]

Table 9.3 Detection limits of vapors

Analyte	Detection limit	Reference
Methanol, ethanol, 2-propanol	10 ppm	Jensenius et al [30]
Toluene, n-octane, ethyl acetate	10 ppm	Jensenius et al [30]
Ethanol	200 ppm	Hierlemann et al [26]
n-octane	5 ppm	Lange et al [33]
Ethanol	14 ppm	Fadel et al [19]
Ethanol	30 ppm	Lochon et al [36]
Butanol	0.19 ppm	Then et al [67]
n-octane	0.6 ppm	Then et al [67]
Toluene	0.38 ppm	Then et al [67]

Table 9.4 Detection limits of Explosives

Analyte	Detection limit	Reference
PETN	1400 ppt	Pinnaduwage et al [49]
RDX	290 ppt	Pinnaduwage et al [49]
DNT	300 ppt	Pinnaduwage et al [54]

Table 9.5 Detection limits of gas pressure and flow

Technique	Measured	Reference
Cantilever in cantilever, pressure	1.33-133 mbar	Brown et al [8]
Cantilever in cantilever, pressure	20-1933 mbar	Brown et al [9]
Resonant response, pressure	10^{-5} – 1000 mbar	Mertens et al [39]
Piezoelectric bimorph, pressure	0.1 – 8.5 bar	Mortet et al [41]
Acousto-optical, pressure	0.1 mbar	Sievilä et al [63]
Bending beam, flow	0.07 m/s	Su et al [66]

Table 9.6 Metal oxide sensors

Gas	Detection limit	Reference
CO	15 ppm	Comini et al [14]
NO_2	200 ppb	Comini et al [14]
NO_2	5 ppm	Penza et al [45]
H_2S	1 ppm	Penza et al [45]
NO	10 ppm	Penza et al [45]
CH_4	1 ppm	Penza et al [45]
SO_2	1 ppm	Penza et al [45]
Ethanol	1000 ppm	Lee et al [35]
Methanol	200 ppm	Lee et al [35]
Toluene	100 ppm	Lee et al [35]
Acetone	200 ppm	Lee et al [35]
Benzene	10 ppm	Lee et al [35]

Table 9.7 Surface acoustic wave sensors

Vapor	Detection range	Reference
Methanol	15 – 130 ppm	Penza et al [46]
Acetone	50 – 250 ppm	Penza et al [46]
Propanol	5 – 70 ppm	Penza and Cassano [47]

Table 9.8 Detection of gases with FET sensors (after Spetz [64])

Gas	Low concentration	High concentration
CO_2	3%	9%
CO	50 ppm	250 ppm
O_2	6%	12%
NO	200 ppm	1000 ppm
C_3H_6	130 ppm	260 ppm
H_2O vapor	2%	2%

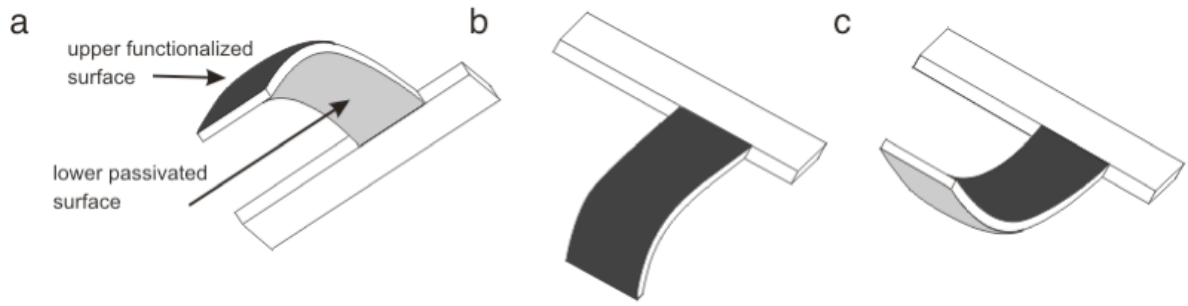

Lang – Cantilever based gas sensing, Figure 1

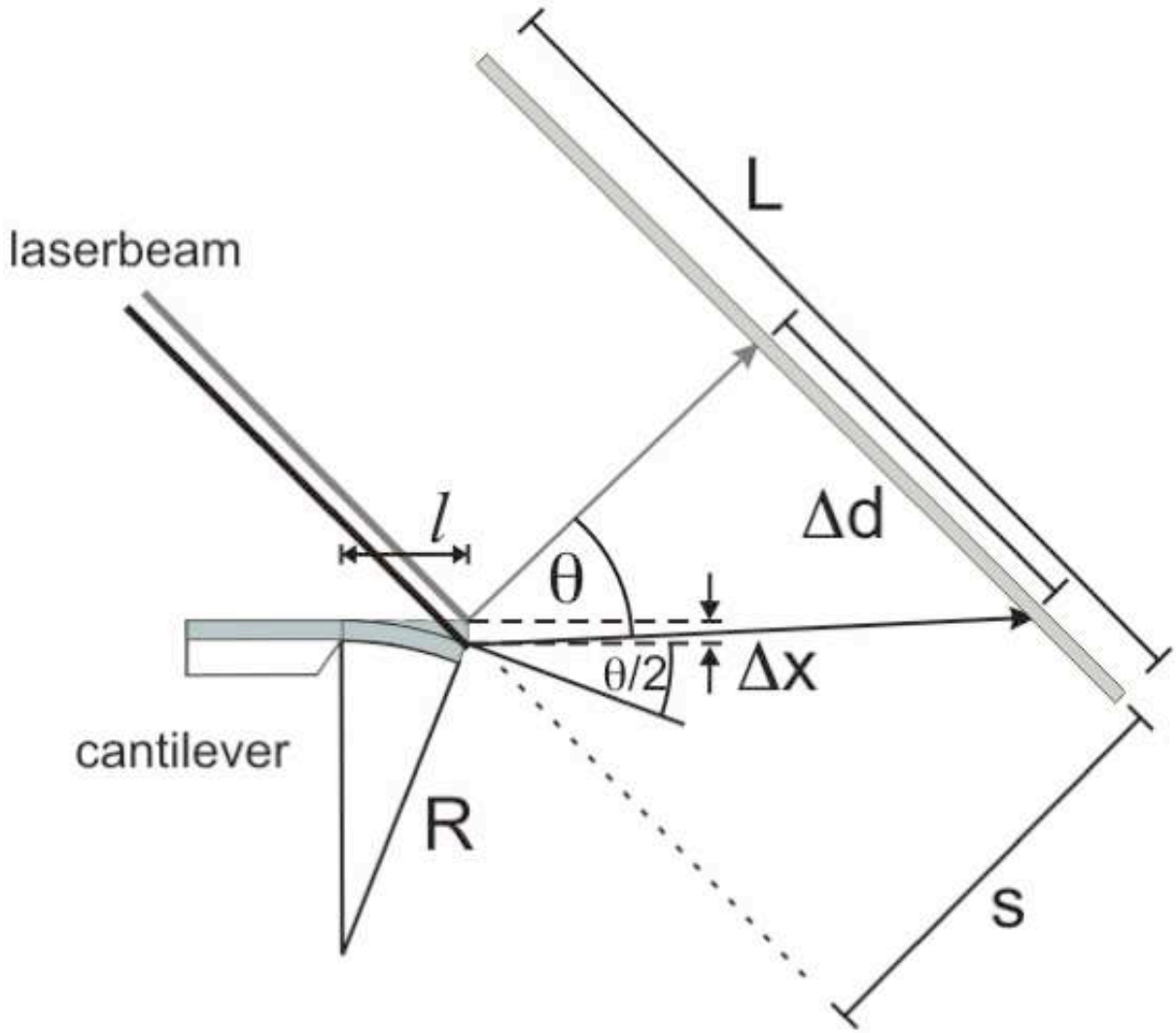

Lang – Cantilever based gas sensing, Figure 2

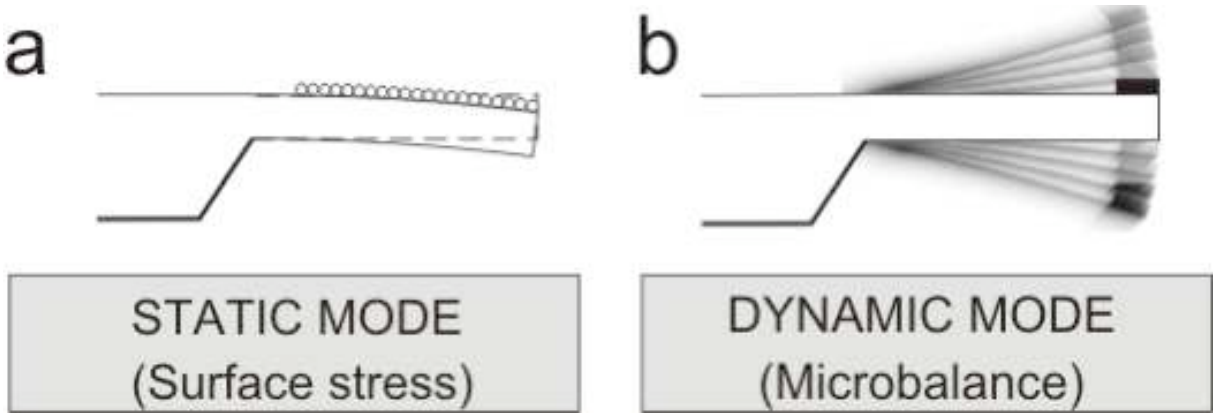

Lang – Cantilever based gas sensing, Figure 3

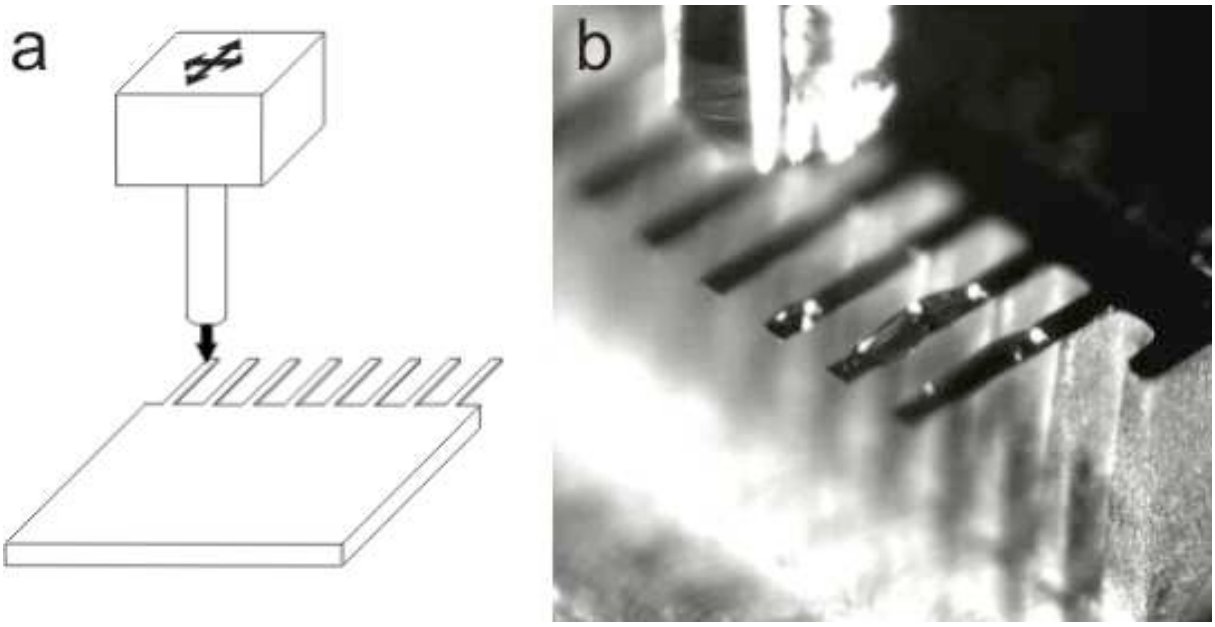

Lang – Cantilever based gas sensing, Figure 4

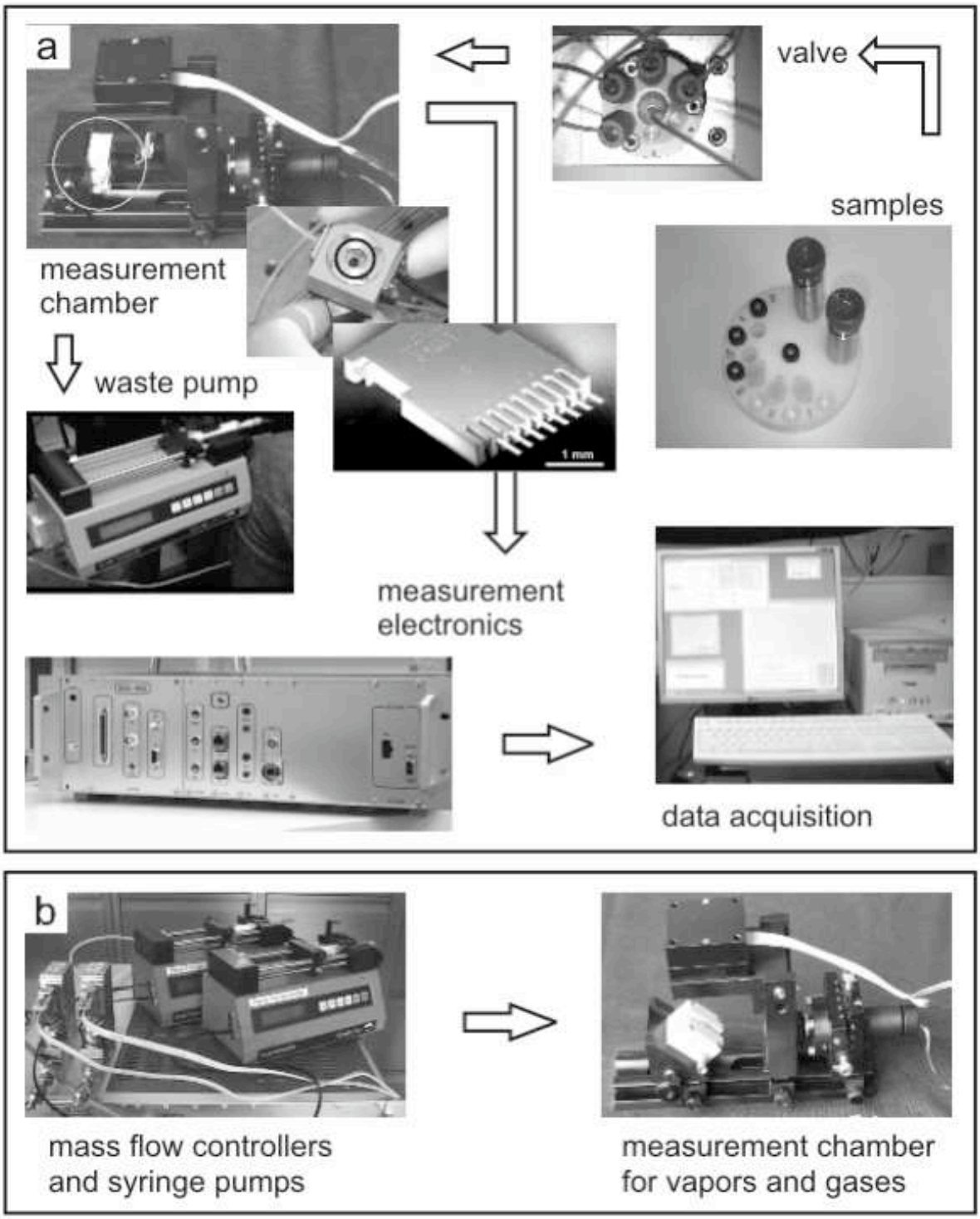

Lang – Cantilever based gas sensing, Figure 5

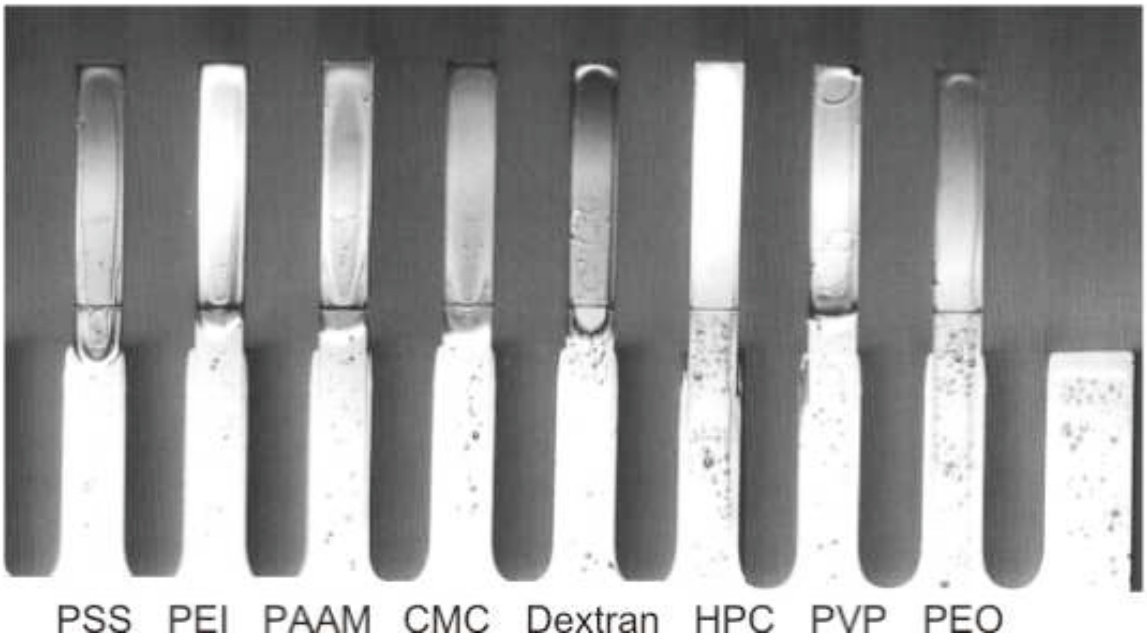

Lang – Cantilever based gas sensing, Figure 6

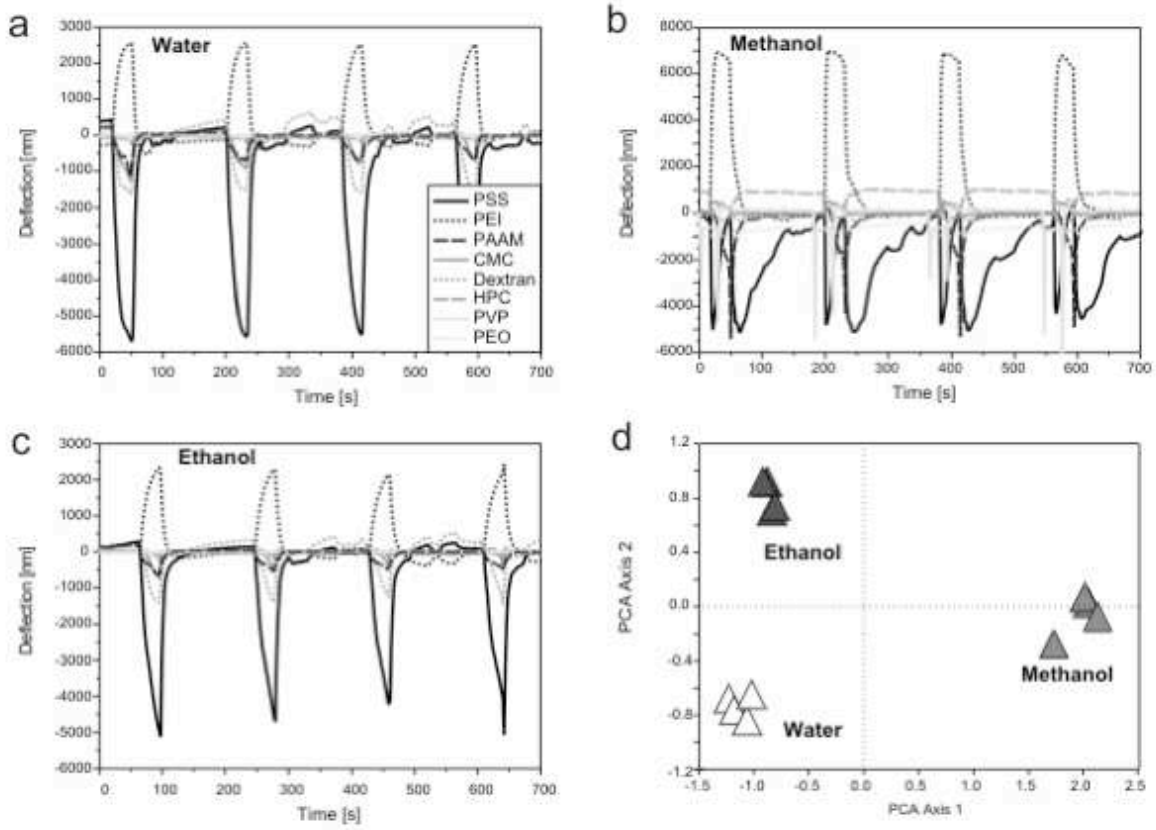

Lang – Cantilever based gas sensing, Figure 7